Raman and Fluorescence Spectra of Size-Selected, Matrix-Isolated C₁₄ and C₁₈ Neutral Carbon Clusters

Gregory A. Rechtsteiner,[†] Christian Felix,[†,‡] Adina K. Ott,[†] Oliver Hampe,[†,§] Richard P. Van Duyne,[†] Martin F. Jarrold,*,[†] and Krishnan Raghavachari[∥]

Department of Chemistry, Northwestern University, 2145 Sheridan Road, Evanston, Illinois 60208-3113, and Bell Laboratories, Lucent Technologies, 600 Mountain Avenue, Murray Hill, New Jersey 07974-0636

The surface plasmon polariton-enhanced Raman spectra of size-selected, matrix-isolated C_{14} neutral clusters are presented along with the calculated vibrational frequencies for the ring and linear chain isomers. The Raman spectra show resonance enhancement over a range of excitation wavelengths from 457.9 to 514.5 nm. The measured vibrational spectra are most consistent with the linear chain isomer. In addition, fluorescence spectra of neutral, mass-selected C_n ($n = 14$ and 18) clusters are presented. The isolated C_{14} clusters display strong fluorescence with vibrational structure between 520 and 700 nm. The origins of the observed fluorescence for both C_{14} and C_{18} are investigated using the ZINDO/S, CIS, and TD-B3LYP methods.

Introduction

An enormous effort has been devoted to understanding the structures and properties of pure carbon clusters.[1,2] Despite this considerable effort, experimental measurements on neutral carbon clusters with more than a few atoms are still limited. Results from infrared spectroscopy[3–5] and surface-enhanced Raman spectroscopy[6,7] are available for neutral carbon clusters, but few experiments have been performed for molecules larger than C_{13}. The linear isomers of neutral C_4 to C_{10} have been verified by ESR measurements in neon matrixes.[8] In addition, electronic absorption spectra of matrix-isolated neutral C_n clusters[9,10] have produced evidence of linear chain structures for C_4–C_{10} and of cyclic structures for C_{10}–C_{14} neutral species. Recently, Krätschmer and co-workers have reported the fluorescence spectrum of neutral C_3 molecules isolated in an argon matrix; however, no mass selection was used during the cluster deposition.[11]

Previously, we presented the first vibrational spectra of mass-selected, matrix-isolated C_{16}, C_{18}, and C_{20} neutral clusters. These spectra were recorded using surface plasmon polariton (SPP) enhanced Raman spectroscopy.[7] The observed spectra were found to be most consistent with linear chain structures. In addition, strong fluorescence (between 620 and 760 nm) was observed from C_{18} when excited with several argon ion laser lines. No fluorescence was detected from C_{16} or C_{20}.

In this paper, we present the SPP Raman spectra of mass-selected, matrix-isolated C_{14} neutral atomic clusters as well as the calculated vibrational frequencies for the ring and linear chain isomers. Similar to our previous studies of C_{16}, C_{18}, and C_{20}, the Raman spectrum for C_{14} appears to be most consistent with a linear chain structure. In addition, the first fluorescence spectra of neutral, mass-selected C_n clusters are reported: C_{14} clusters, like C_{18}, display strong fluorescence between 520 and 700 nm when excited with an argon ion laser. The origins of the observed fluorescence from C_{14} and C_{18} have been investigated using the ZINDO/S, configuration interaction-singles (CIS) and time-dependent Becke 3-parameter—Lee—Yang—Parr (TD-B3LYP) density functional methods.

Experimental Methods

The experimental apparatus has been described previously.[12,13] Briefly, carbon cluster cations are created by laser ablation (308 nm, 100 Hz) of a graphite rod in a continuous flow of He buffer gas (99.9999%) at ~15 Torr. A 1 kV electron beam is injected into the buffer gas flow to enhance the production of cations. The cluster ions are focused into a low energy beam, injected into a quadrupole mass spectrometer for size selection, and passed through a double-bend quadrupole deflector into the ultrahigh vacuum (UHV) chamber. Following the deposition of a 50 Å N_2 buffer layer, carbon cluster ions are codeposited with N_2 onto a silver-coated (550 Å thickness) hemicylindrical sapphire prism cooled to 10 K. The cluster ions are deposited at ~25 eV. The measured spectra are independent of the deposition energy, indicating that fragmentation did not occur during deposition. The ions in the matrix are neutralized by low-energy electrons from a hot filament during deposition. The sample contains approximately 5×10^{11} clusters in an 1100 Å thick matrix. After cluster deposition, a 2 μm thick capping layer of N_2 is added to provide the correct conditions for the surface plasmon enhancement and to protect the cluster sample from contamination.

The 457.9, 488.0, and 514.5 nm lines of an argon ion laser (Spectra-Physics model 164) and 635 and 647 nm from an argon ion laser (Spectra-Physics model 2060) pumped dye laser (Coherent model 590) using DCM are used for excitation. Raman scattered light is focused into a triple grating spectrometer (SPEX Triplemate) with either 600 or 1800 gr/mm gratings and is imaged onto a charge-coupled device (CCD) detector (Princeton Instruments model LN/ccd-512). Data acquisition times range from 60 to 300 s at laser powers between 10 and 200 mW.

[†] Northwestern University.
[‡] Current address: Institut de Physique Experimentale, EPFL, Laussane, Switzerland.
[§] Current address: Institut für Nanotechnologie, Karlsruhe, Germany.
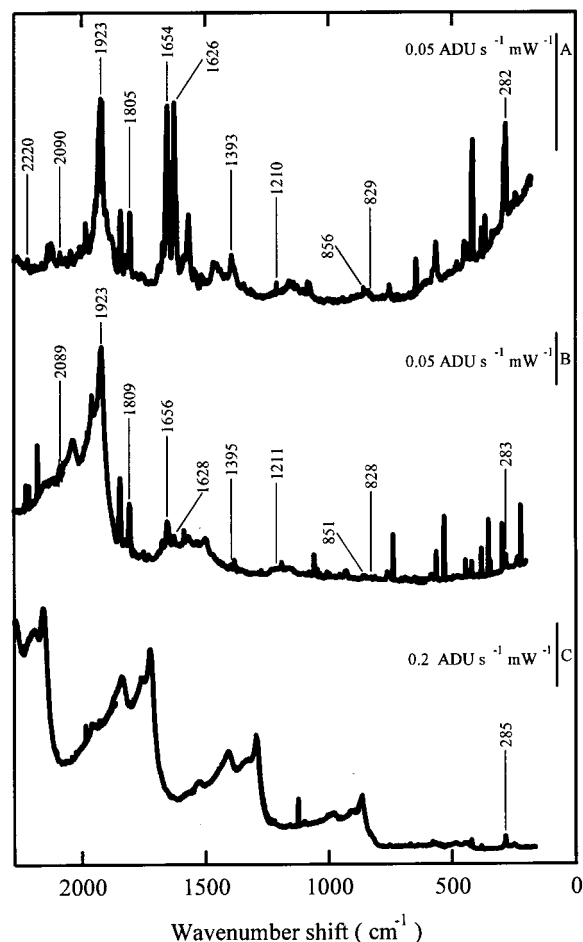[∥] Lucent Technologies.

Figure 1. Raman spectra of matrix-isolated, neutral C_{14} clusters over the $150-2250$ cm^{-1} range for excitation wavelengths of 457.9 (A), 488.0 (B), and 514.5 (C) nm.

Experimental Results

Figure 1 shows the Raman signal for C_{14} in analog-to-digital converter units (ADU s^{-1} mW^{-1}) at excitation wavelengths of 457.9 (A), 488.0 (B), and 514.5 (C) nm as a function of wavenumber shift (in cm^{-1}). The spectra exhibit resonance enhancement as shown by the change in intensity of the features at 1627 and 1655 cm^{-1} as the incident wavelength changes. Fluorescence from C_{14} was observed between 520 and 700 nm at excitation wavelengths of 457.9, 488.0, and 514.5 nm. At excitation wavelengths of 635 and 647 nm, very weak Raman signals with shifts between 200 and 600 cm^{-1}, and weak fluorescence peaks between the excitation wavelength and 700 nm were observed.

The experimental frequencies reported in Table 1 were determined by matching peaks present at nearly all of the excitation wavelengths. Previously, we reported[7] systematic shifts in the frequencies for the series of peaks at 250, 223, and 198 cm^{-1} for C_{16}, C_{18}, and C_{20} clusters, respectively. This progression suggests that the spectra do not result from a isomers analogous to a C_{20} bowl or cage isomer since such structures are not feasible for C_{16} and C_{18}. The observed spectra were found to most closely agree with those calculated for linear chains. This progression is continued by the C_{14} peak at 282 cm^{-1}. The first overtone of this feature is also present at 564 cm^{-1}. The addition of the C_{14} data to this frequency set indicates that the four clusters share similar structures and suggests that the Raman spectra of C_{14} are probably due mainly to a linear chain isomer. As noted previously, the chain isomers do not

TABLE 1: Vibrational Parameters for C_{14}

$C_{14}{}^{a}$	$C_{14}(D_{7h})^{b}$	$C_{14}(D_{4h})^{b,c}$
		58 (Π_g)
	96 (E_2')	
282		
		171 (Π_g)
		295 (Σ_g)
		297 (Π_g)
	342 (A_1')	
		455 (Π_g)
	489 (A_1')	
	536 (E_2')	515 (Π_g)
	602 (E_1'')	637 (Π_g)
829		
851		850 (Σ_g)
	1199 (E_2')	
1211		
		1351 (Σ_g)
1394		
1627		
1655		
		1791 (Σ_g)
1807		
		1884 (Σ_g)
1926		
2089		2061 (Σ_g)
	2101 (E_2')	
		2180 (Σ_g)
2218		

a Experimental SPP-enhanced Raman frequencies in cm^{-1}. *b* Calculated Raman-active frequencies in cm^{-1}. *c* Cumulene chain isomer.
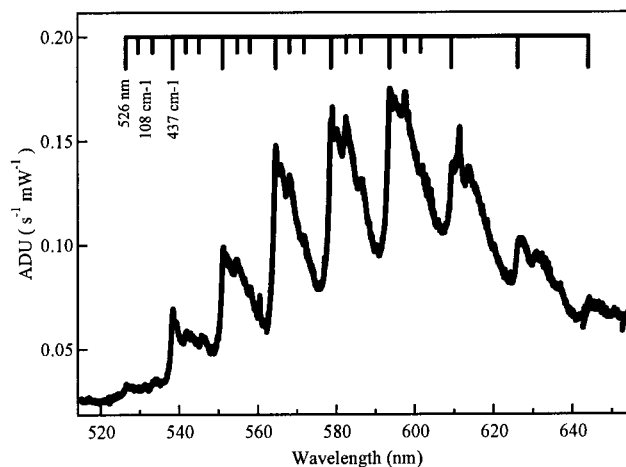

Figure 2. Fluorescence spectra of martrix-isolated, neutral C_{14} clusters over the $515-655$ nm range at an excitation wavelength of 457.9 nm. The origin is at 526 nm, and sticks indicate the vibrational progression at spacings of 108 and 437 cm^{-1}.

seem to account for all of the observed features. This may indicate the presence of another isomer, for example, a monocyclic ring.

Figures 2 and 3 show the fluorescence spectra acquired for C_{14} and C_{18}, respectively. The measured fluorescence peak origins reported in Table 2 were determined by matching peaks at excitations wavelengths of 457.9, 488.0, and 514.5 nm. The frequencies of the progressions were determined using the same method. The C_{14} spectrum shows an electronic transition at 526 nm which serves as an origin for progressions that occur with spacings of 108 and 437 cm^{-1}. Similarly, the C_{18} spectrum shows an electronic transitions at 624 and 666 nm (1006 cm^{-1} separation), which are origins for progressions that occur with spacings of 408 and 877 cm^{-1} and 440 and 877 cm^{-1}, respectively. The assignment of the peaks at 624 and 666 nm to transitions from two different excited electronic states is supported by calculations for C_6 that show close-lying electronic states ($1200-2300$ cm^{-1}).[14]

Matrix-Isolated Neutral Carbon Clusters

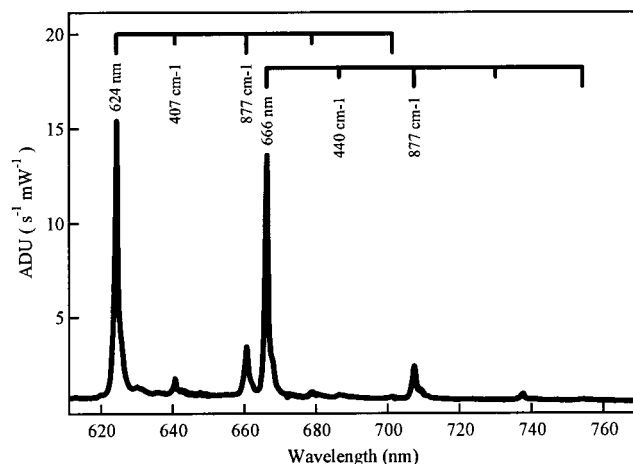*J. Phys. Chem. A, Vol. 105, No. 13, 2001* **3031**

Figure 3. Fluorescence spectra of martrix-isolated, neutral C_{18} clusters over the 610−770 nm range at an excitation wavelength of 457.9 nm. The origins are at 624 and 666 nm; sticks indicate the vibrational progressions at spacings of 407 and 877 cm^{-1} and 440 and 877 cm^{-1}, respectively.

TABLE 2: Electronic Transition Parameters for C_{14} and C_{18}

cluster	expt^a	ZINDO/S^b	CIS^b	TD-B3LYP^b
Cumulene Chains				
C_{14} $D_{\infty h}$	526	446 (0.0425)^c	410 (5.7300)^c	784 (0.0001)^c
			440 (0.0115)	891 (0.0004)
C_{16} $D_{\infty h}$		480 (0.0547)	435 (0.0116)	779 (0.0001)
			457 (6.4178)	994 (0.0004)
C_{18} $D_{\infty h}$	624	513 (0.0815)	430 (0.0118)	773 (0.0001)
	666		503 (6.8159)	1097 (0.0004)
C_{20} $D_{\infty h}$		542 (0.1008)	547 (7.1074)	769 (0.0001)
				1195 (0.0004)
Cumulene Rings				
C_{14} D_{7h}	526	542 (0.0096)	417 (0.0048)	416 (0.0004)
			429 (0.0071)	427 (0.0001)
C_{16} C_{8h}		562 (0.0036)	521 (0.0013)	386 (0.0001)
			545 (0.0043)	
C_{18} D_{9h}	624	749 (0.0019)	555 (0.0054)	509 (0.0001)
	666			543 (0.0001)
C_{20} C_{10h}		470 (0.0003)	539 (0.0007)	457 (0.0001)
		516 (0.0006)	574 (0.0012)	

^{a} Experimental fluorescence peak positions in nanometers. ^{b} Calculated orbitally allowed electronic transition values in nanometers. ^{c} Calculated oscillator strength.

Theoretical Methods

The geometry optimization and frequency calculations were performed using GAUSSIAN 98W (Revision A.7),[15] using the B3LYP (Becke 3-parameter−Lee−Yang−Parr) functional[16] and the cc-pVDZ (correlation consistent polarized valence double-ζ, a [3s2p1d] contraction of the (9s4p1d) primitive set) basis set.[17] The B3LYP/cc-pVDZ harmonic frequencies were uniformly scaled down by 2% to account for the systematic overestimation that results from the neglect of anharmonic effects.

Excited electronic state calculations were performed with stationary state structures obtained from geometry optimizations using the B3LYP functional and the 6-31G* basis set.[18−20] The ZINDO/S calculations were performed using ZINDO, a comprehensive semiempirical SCF/CI package developed by Zerner and co-workers.[21−23] The CIS[24] and TD-B3LYP[25−27] calculations were performed using GAUSSIAN 98W (revision A.7), using the 6-31G* basis set.

Theoretical Results

The lowest energy ring or chain isomer found for the C_{14} cluster is a D_{7h} cumulene ring, with a $D_{\infty h}$ cumulene chain lying

3.0 eV higher in energy. Optimizations performed with polyacetylene ring or chain structures as the initial geometries converged to cumulene species identical to those above. Table 1 shows the measured vibrational frequencies and the predicted Raman-active frequencies predicted for the ring and linear chain isomers of C_{14} by density functional theory.

Table 2 shows the predicted, orbitally allowed vertical electronic transitions (excitation) for the ring and linear chain isomers of C_{14} and C_{18} from the ZINDO/S, CIS, and TD-B3LYP calculations. The electronic configurations of neutral $D_{\infty h}$ C_{14} and C_{18} cumulene chains are ... $(\pi_u)^2$, resulting in $^3\Sigma_g^-$ ground states. The expected electronic transitions for neutral carbon chains with even numbers correspond to $^3\Sigma_u^- - X\ ^3\Sigma_g^-$ and $^3\Pi_u - X\ ^3\Sigma_g^-$ symmetry. The electronic configurations of neutral cumulene D_{7h} C_{14} and D_{9h} C_{18} rings are ... $(e'')^4$, resulting in $^1A_1'$ ground states. The expected electronic transitions for the neutral carbon C_{14} and C_{18} rings correspond to $^1E_1'' - X^1A_1'$ symmetry.

Discussion

From comparison of the measured frequencies and the calculated frequencies for the C_{14} ring and linear chain isomers (see Table 1) it appears that the chain structure gives the closest matches to the experimental. The frequencies at 282 cm^{-1} and at 851 cm^{-1} match the first two totally symmetric fundamentals calculated for the chain isomers of C_{14}. As in the previous studies of C_{16}, C_{18}, and C_{20}, definitive determination of the fundamental frequencies of C_{14} from the spectra is complicated by the resonance enhancement and in some cases the strong fluorescence of the cluster. Excitation with longer wavelengths reduced the resonance contribution; however, a corresponding decrease in signal-to-noise ratio and the presence weak fluorescence features only allow for identification of the 282 cm^{-1} fundamental vibration.

The measured fluorescence origins are compared in Table 2 to the calculated, orbitally allowed vertical electronic transitions for the ring and linear chain isomers. For the linear chain isomers, the results from the ZINDO/S and CIS calculations are in qualitative agreement and strongly differ from the results of the TD-B3LYP calculations. The TD-B3LYP calculations are strongly shifted toward the infrared region of the spectrum and have two different sets of transitions: one that increases in wavelength with increasing cluster size and one that decreases. The transitions predicted for the linear chain isomers by ZINDO/S, CIS, and one set of transitions from the TD-B3LYP calculations show a shift toward longer wavelengths as the carbon chain gets longer. This trend is in qualitative agreement with the experimental observations for C_{14} and C_{18}. Such a shift is also apparent in the electronic spectra of carbon chains C_4, C_6, C_8, and C_{10} reported by Maier and co-workers.[9] The ZINDO/S and CIS results are in qualitative agreement with a second state of $^3\Sigma_u^-$ symmetry with large oscillator strengths that has been reported by Maier.[9] However, the ZINDO/S and CIS calculations suggest that fluorescence spectra should be observed from C_{16} and C_{20} clusters, but as reported previously, no fluorescence is observed from C_{16} and C_{20}.

The results of the calculations on the ring isomers using the three methods are in qualitative agreement with each other (with the exception of the ZINDO/S predictions for D_{9h} C_{18}), but they are not in agreement with the experimental observations. The transitions predicted by the ZINDO/S calculations suggest that fluorescence should be observed from all four cluster species. The CIS calculations predict transitions that suggest fluorescence should not be seen from C_{14} but should be seen from C_{16}, C_{18},

and C_{20}. The transitions predicted by the TD-B3LYP calculations suggest that fluorescence should only have been seen from C_{18} and perhaps C_{20}. However, even in these cases, the experimental results are red shifted from the predicted transitions.

The poor agreement between theory and experiment suggests that the observed fluorescence spectra may be due to transitions to orbitally forbidden electronic states that become accessible through vibrational coupling. For a vibronic transition, the transition moment integral has the form

$$M = \int \psi_e^* \psi_{v'}^* \hat{u}_e \psi_e \psi_v \, d\tau_{en} \qquad (1)$$

and the combined electronic−vibration integral must be nonzero for a vibronic transition to be allowed. Any vibration of the molecule with symmetry that makes the integral nonzero can make a transition allowed. Therefore, by the coupling of an orbitally forbidden electronic transition with a vibrational transition of the right symmetry, it is possible that the selection rules can be satisfied and some intensity may be observed. Since the fluorescence results from a downward, vertical electronic transition (in accordance with the Franck−Condon principle), the vibrational structure in the fluorescence spectra are characteristic of vibrations in the ground electronic state.

Potential vibrationally allowed electronic transitions for the chain species are considered first since the observed Raman spectra of C_{14} and C_{18} are found to most closely agree with those calculated for linear chains. The CIS and TD-B3LYP electronic excited-state calculations find several orbitally forbidden transitions to Σ_g, Δ_g, and Δ_u excited states in the 500−700 nm range for C_{14} and C_{18} chains. These orbitally forbidden transitions can become allowed by coupling with vibrational transitions having Σ_u or Π_u, Σ_u or Π_u, or Π_g symmetry, respectively. (The two components of the dipole moment operator, μ_e, for the $D_{\infty h}$ point group are Σ_u and Π_u.)

For a C_{14} linear chain, the CIS and TD-B3LYP calculations find a Δ_u state at 539 nm and a Σ_g state at 545 nm, respectively. For the chain isomer, the B3LYP calculations find a Π_u mode at 109 cm^{-1} and a Π_g mode at 455 cm^{-1}. These are the closest matching vibrations to the vibrational progressions of 108 and 437 cm^{-1} that are present in the fluorescence spectrum for C_{14}. For a C_{18} linear chain, the CIS calculations find Δ_u states at 572 and 740 nm. The TD-B3LYP calculations find a Δ_g state at 609 nm, a Σ_g state at 683 nm, and a Δ_g state at 701 nm. The only feature in the C_{18} Raman spectra that is close to the frequencies observed in the fluorescence spectra (407 and 877 cm^{-1}, origin at 624 nm, and 440 and 877 cm^{-1}, origin at 666 nm) is an unassigned peak at 430 cm^{-1}. For the chain isomer, the closest matching vibrations from the calculations are a Π_g mode at 452 cm^{-1}, a Σ_u mode at 455 cm^{-1}, a Σ_u mode at 884 cm^{-1}, and a Π_g mode at 895 cm^{-1}. The consideration of vibrational coupling results in better agreement between the experimental fluorescence spectra and the electronic excited-state calculations.

The CIS and TD-B3LYP electronic excited-state calculations also find several orbitally forbidden transitions to Σ_g, Δ_g, and Δ_u excited states in the 500−800 nm range for C_{16} and C_{20} chains. As shown above, these orbitally forbidden transitions can become vibrationally allowed. Therefore, the excited-state calculations are not in agreement with the experimental observations which have detected fluorescence from C_{14} and C_{18} clusters but not from C_{16} and C_{20} clusters.

The alternating fluorescence properties may be due to vibrationally allowed electronic transitions of monocyclic ring species present in the matrix. Due to limitations in the Gaussian 98W program, the ring excited-state symmetries cannot be readily determined. However, it should be noted that, for the C_{14} ring isomer, the nearest matching calculated vibrations to the vibrational progressions of 108 and 437 cm^{-1} that are present in the fluorescence spectra are an E_2'' mode at 126 cm^{-1} and a E_3' mode at 427 cm^{-1}. For the C_{18} ring isomer, the nearest matching calculated vibrations to the vibrational progressions of 407 and 877 cm^{-1} and 440 and 877 cm^{-1} are an E_4' mode at 397 cm^{-1}, an E_4'' mode at 415 cm^{-1}, an E_3' mode at 456 cm^{-1}, an A_1' mode at 464 cm^{-1}, an A_2'' mode at 788 cm^{-1}, and a E_2' mode at 976 cm^{-1}. It is plausible that the fluorescence results from ring isomers because theoretical calculations have found that C_{4n+2} (C_{14} and C_{18}) rings have $D_{(n/2)h}$ cumulene ring geometries and C_{4n} (C_{16} and C_{20}) rings have $C_{(n/2)h}$ polyacetylene ring geometries.[7,28,29] The alternating ring structures could explain why fluorescence spectra are seen for C_{14} and C_{18} and not for C_{16} and C_{20}. Conversely, C_n linear chains with even number of carbon atoms all have the same type of cumulene structure.[7,30,28]

In conclusion, the SPP-Raman spectra for size-selected C_{14}, C_{16}, C_{18}, and C_{20} clusters appear to most closely agree with those calculated for linear chains. The most reasonable interpretation of the C_{14} and C_{18} fluorescence is that it results from cumulene rings. However, further theoretical studies of the excited states of C_{14}, C_{16}, C_{18}, and C_{20} isomers are required in order to resolve the discrepancies between experiment and theory.

References and Notes

(1) Weltner, W.; Van Zee, R. J. *Chem. Rev.* **1989**, *89*, 1719−1747.

(2) Van Orden, A.; Provencal, R. A.; Keutsch, F. N.; Saykally, R. J. *J. Chem. Phys.* **1996**, *105*, 6111−6116.

(3) Giesen, T. F.; Van Orden, A.; Hwang, H. J.; Fellers, R. S.; Provencal, R. A.; Saykally, R. J. *Science* **1994**, *265*, 756.

(4) Szczepanski, J.; Ekern, S.; Vala, M. *J. Phys. Chem. A* **1997**, *101*, 1841−1847.

(5) Wang, S. L.; Rittby, C. M. L.; Graham, W. R. M. *J. Chem. Phys.* **1997**, *107*, 7025−7033.

(6) Haslett, T. L.; Fedrigo, S.; Moskovits, M. *J. Chem. Phys.* **1995**, *103*, 7815.

(7) Ott, A. K.; Rechtsteiner, G. A.; Felix, C.; Hampe, O.; Jarrold, M. F.; Van Duyne, R. P. *J. Chem. Phys.* **1998**, *109*, 9652−9655.

(8) Van Zee, R. J.; Ferrante, R. F.; Zeringue, K. J.; W Weltner, J.; Ewing, D. W. *J. Chem. Phys.* **1988**, *88*, 3465−3474.

(9) Maier, J. P. *J. Phys. Chem. A* **1998**, *102*, 3462−3469.

(10) Grutter, M.; Wyss, M.; Riaplov, E.; Maier, J. P.; Peyerimhoff, S. D.; Hanrath, M. *J. Chem. Phys.* **1999**, *111*, 7397−7401.

(11) Cermak, I.; Forderer, M.; Cermakova, I.; Kalhofer, S.; Stopka-Ebeler, H.; Monninger, G.; Kratschmer, W. *J. Chem. Phys.* **1998**, *108*, 10129−10142.

(12) Honea, E. C.; Ogura, A.; Murray, C. A.; Raghavachari, K.; Sprenger, W. O.; Jarrold, M. F.; Brown, W. L. *Nature* **1993**, *366*, 42−44.

(13) Honea, E. C.; Ogura, A.; Peale, D. R.; Felix, C.; Murray, C. A.; Raghavachari, K.; Sprenger, W. O.; Jarrold, M. F.; Brown, W. L. *J. Chem. Phys.* **1999**, *110*, 12161−12172.

(14) Parasuk, V.; Almlof, J. *J. Chem. Phys.* **1989**, *91*, 1137−1141.

(15) Frisch, M. J.; Trucks, G. W.; Schlegel, H. B.; Scuseria, G. E.; Robb, M. A.; Cheeseman, J. R.; Zakrzewski, V. G.; J A Montgomery, J.; Stratmann, R. E.; Burant, J. C.; Dapprich, S.; Millam, J. M.; Daniels, A. D.; Kudin, K. N.; Strain, M. C.; Farkas, O.; Tomasi, J.; Barone, V.; Cossi, M.; Cammi, R.; Mennucci, B.; Pomelli, C.; Adamo, C.; Clifford, S.; Ochterski, J.; Petersson, G. A.; Ayala, P. Y.; Cui, Q.; Morokuma, K.; Malick, D. K.; Rabuk, A. D.; Raghavachari, K.; Foresman, J. B.; Cioslowski, J.; Ortiz, J. V.; Stefanov, B. B.; Liu, G.; Liashenko, A.; Piskorz, P.; Komaromi, I.; Gomperts, R.; Martin, R. L.; Fox, D. J.; Keith, T.; Al-Laham, M. A.;

Matrix-Isolated Neutral Carbon Clusters

J. Phys. Chem. A, Vol. 105, No. 13, 2001 **3033**

Peng, C. Y.; Nanayakkara, A.; Gonzalez, C.; Challacombe, M.; Gill, P. M. W.; Johnson, B.; Chen, W.; Wong, M. W.; Andres, J. L.; Gonzalez, C.; Head-Gordon, M.; Replogle, E. S.; Pople, J. A. *Gaussian 98*, revision A.3; Gaussian, Inc.: Pittsburgh, PA, 1998.

(16) Becke, A. D. *J. Chem. Phys.* **1993**, *98*, 5648−5652.

(17) Dunning, T. H. *J. Chem. Phys.* **1989**, *90*, 1007−1023.

(18) Ditchfield, R.; Hehre, W. J.; Pople, J. A. *J. Chem. Phys.* **1971**, *54*, 724.

(19) Hehre, W. J.; Ditchfield, R.; Pople, J. A. *J. Chem. Phys.* **1972**, *56*, 2257.

(20) Frisch, M. J.; Pople, J. A.; Binkley, J. S. *J. Chem. Phys.* **1984**, *80*, 3265.

(21) Ridley, J. E.; Zerner, M. C. *Theor. Chim. Acta* **1976**, *42*, 223.

(22) Bacon, A. D.; Zerner, M. C. *Theor. Chim. Acta* **1979**, *53*, 21.

(23) Zerner, M. C.; Loew, G. H.; Kirchner, R. F.; Mueller-Westerhoff, U. T. *J. Am. Chem. Soc.* **1980**, *102*, 589.

(24) Foresman, J. B.; Head-Gordon, M.; Pople, J. A.; Frisch, M. J. *J. Phys. Chem.* **1992**, *96*, 135.

(25) Bauernschmitt, R.; Ahlrichs, R. *Chem. Phys. Lett.* **1996**, *256*, 454.

(26) Casida, M. E.; Jamorski, C.; Casida, K. C.; Salahub, D. R. *J. Chem. Phys.* **1998**, *108*, 4439−4449.

(27) Stratmann, R. E.; Scuseria, G. E.; Frisch, M. J. *J. Chem. Phys.* **1998**, *109*, 8218−8224.

(28) Martin, J. M. L.; El-Yazal, J.; Francois, J.-P. *Chem. Phys. Lett.* **1995**, *242*, 570−579.

(29) Martin, J. M. L.; El-Yazal, J.; Francois, J.-P. *Chem. Phys. Lett.* **1996**, *248*, 345−352.

(30) Fan, Q.; Pfeiffer, G. V. *Chem. Phys. Lett.* **1989**, *162*, 472−478.